An iron-induced nitric oxide burst precedes ubiquitin-dependent protein degradation for Arabidospsis Atfer1 ferritin gene expression.

Nicolas Arnaud, Iréne Murgia, Jossia Boucerez, Jean-François Briat, Françoise Cellier, Frédéric Gaymard

THE JOURNAL OF BIOLOGICAL CHEMISTRY VOL. 281, NO. 33, pp. 23579–23588, August 18, 2006

An Iron-induced Nitric Oxide Burst Precedes Ubiquitin-dependent Protein Degradation for *Arabidopsis AtFer1* Ferritin Gene Expression*

Received for publication, March 7, 2006, and in revised form, May 2, 2006 Published, JBC Papers in Press, June 16, 2006, DOI 10.1074/jbc.M602135200

Nicolas Arnaud[‡1], Irene Murgia[§], Jossia Boucherez[‡], Jean-François Briat[‡], Françoise Cellier[‡], and Frédéric Gaymard[‡2]

From the [‡]Laboratoire de Biochimie et Physiologie Moléculaire des Plantes, UMR 5004 Agro-M/CNRS/INRA/UMII, Bat 7, 2 place Viala, 34060 Montpellier Cedex 1, France and the [§]Sezione di Fisiologia e Biochimica delle Piante, Dipartimento di Biologia, Università degli Studi di Milano, via Celoria 26, 20133 Milano, Italy

Ferritins play an essential role in iron homeostasis by sequestering iron in a bioavailable and non-toxic form. In plants, ferritin mRNAs are highly and quickly accumulated in response to iron overload. Such accumulation leads to a subsequent ferritin protein synthesis and iron storage, thus avoiding oxidative stress to take place. By combining pharmacological and imaging approaches in an *Arabidopsis* cell culture system, we have identified several elements in the signal transduction pathway leading to the increase of *AtFer1* transcript level after iron treatment. Nitric oxide quickly accumulates in the plastids after iron treatment. This compound acts downstream of iron and upstream of a PP2A-type phosphatase to promote an increase of *AtFer1* mRNA level. The *AtFer1* gene transcription has been previously shown to be repressed under low iron conditions with the involvement of the *cis*-acting element iron-dependent regulatory sequence identified within the *AtFer1* promoter sequence. We show here that the repressor is unlikely a transcription factor directly bound to the iron-dependent regulatory sequence; such a repressor is ubiquitinated upon iron treatment and subsequently degraded through a 26 S proteasome-dependent pathway.

As the major cofactor of proteins involved in essential processes like photosynthesis, respiration, DNA replication, or nitrogen fixation, iron is an essential element for life. Nonetheless, in the free ionic form, iron is toxic as it can catalyze the formation of reactive oxygen species through the Fenton reaction. These reactive oxygen species damage the cell membranes, DNA, and proteins (1, 2). Thus, iron homeostasis has to be tightly regulated, to avoid starvation that impairs the metabolism, and to avoid excess that may lead to cell death. Iron homeostasis is strongly dependent on ferritins, which are iron-storage proteins, found in bacteria, animals, and plants. Plant and animal ferritin structures are very similar, and are formed by 24 subunits arranged to form a hollow sphere able to sequester iron in a non-toxic and bioavailable form (3).

In animals, ferritin synthesis is mainly regulated at the post-transcriptional level (3, 4). Ferritin mRNAs contain iron-responsive elements in their 5′-untranslated regions that function as binding sites for two related *trans*-acting factors, namely iron regulatory proteins IRP1 and IRP2. When bound to the iron-responsive element in the ferritin mRNA, the IRP inhibit translation of the transcript (4). IRP1 is a bifunctional protein that when iron is abundant possesses a 4Fe-4S cluster and acts as cytoplasmic aconitase. When iron levels are low, the 4Fe-4S cluster disassembles and the apoprotein acquires IRP[3] activity, thus repressing ferritin translation. High levels of iron lead to the 4Fe-4S cluster reconstitution and therefore the protein aconitase activity. In contrast to IRP1, IRP2 cannot assemble a iron-sulfur cluster and lacks aconitase activity. IRP2 shares about 60% amino acid sequence identity with IRP1, but differs only in having a 73-amino acid insertion in its N-terminal region. This region contains a cysteine-rich sequence responsible for targeting the protein for degradation via the ubiquitin-proteasome pathway when cellular iron level is high (5, 6). NO has been shown to play an important role in iron metabolism by modulating both IRP1 and IRP2 activities (7, 8). Exposure to $NO^{\cdot}$ was shown to disassemble the iron-sulfur cluster of IRP1, promoting binding to ferritin mRNA (4, 9). By contrast, IRP2 binding to iron-responsive elements is negatively regulated by NO (10–12). An oxidized form of NO, the nitrosonium ion NO^{+} (11, 13) may cause the *S*-nitrosylation of a cysteine found in the Fe^{2+}-dependent degradation domain of IRP2, leading to a subsequent and specific down-regulation of IRP2 by the ubiquitin/26 S proteasome pathway (14, 15).

Plant ferritins can be found in mitochondria (16), but in contrast to animal cells, they have never been observed in the cyto-

* This work was supported by Institut National de la Recherche Agronomique and Centre National de la Recherche Scientifique, Action Concertée Incitative "Biologie Cellulaire Moléculaire et Structurale" Grant BCMS166 from the Ministère de l'Education Nationale, de l'Enseignement Supérieur et de la Recherche. The costs of publication of this article were defrayed in part by the payment of page charges. This article must therefore be hereby marked "*advertisement*" in accordance with 18 U.S.C. Section 1734 solely to indicate this fact.

[1] Supported by a thesis fellowship from the Ministère de l'Education Nationale, de l'Enseignement Supérieur et de la Recherche.

[2] To whom correspondence should be addressed. Tel.: 33-499-61-29-32; Fax: 33-467-52-57-37; E-mail: gaymard@ensam.inra.fr.

[3] The abbreviations used are: IRP, iron regulatory protein; cPTIO, 2-(4-carboxyphenyl)-4,5-dihydro-4,4,5,5-tetramethyl-1*H*-imidazol-1-yl-oxy-3-oxide; DAF-FM DA, 4-amino-5-methylamino-2′,7′-difluorofluorescein diacetate; IDRS, iron-dependent regulatory sequence; L-NMMA, N^{G}-monomethyl-L-arginine; PP2A, protein phosphatase type 2A; OA, okadaic acid; SNP, sodium nitroprusside; NO, nitric oxide; MES, 4-morpholineethanesulfonic acid; Pipes, 1,4-piperazinediethanesulfonic acid; DTT, dithiothreitol; NR, nitrate reductase; NOS, nitric-oxide synthase; ABA, abscisic acid.

plasm, and their main location is in the plastids (17). In addition, their synthesis is regulated at the transcriptional level in response to iron excess (17, 18), and not at the translational level as described above for animal cells. In plants, ferritin mRNA abundance has been shown to be regulated by several environmental factors including iron (17, 19–21), H_2O_2 (22), photoinhibition (23), pathogen attacks (24), by the stress hormone ABA (25), and by NO donors or scavengers (26, 27). Experiments based on serial deletions and site-directed mutagenesis of maize *ZmFer1* and *Arabidopsis AtFer1* ferritin promoter sequences allowed to identify a 15-bp *cis*-acting element necessary for the iron-dependent regulation of the transcription of these genes (18). This sequence, named IDRS, for iron-dependent regulatory sequence, has been shown to be involved in the repression of *ZmFer1* and *AtFer1* gene expression under iron-deficient conditions (18, 28). Thus, iron addition leads to the de-repression of *ZmFer1* and *AtFer1* gene expression rather than to their induction.

Despite the growing number of physiological conditions reported to date leading to plant ferritin synthesis, little is known about the regulatory molecules acting downstream of iron. By using an *Arabidopsis* cell culture system, we show in this work that iron excess and oxidative stress, mimicked by exogenous H_2O_2 application, promote *AtFer1* gene expression through two independent and additive pathways. We show also that iron application leads to a rapid NO burst in the plastids of the cell. This NO accumulation, which does not involve NOS1 nor nitrate reductase activities, is leading to *AtFer1* de-repression. The factor that represses *AtFer1* transcription under iron-deficient conditions is ubiquitinated and degraded by a 26 S proteasome-dependent pathway after iron application. This repressor is not a transcription factor directly bound to the IDRS present in the *AtFer1* promoter region.

EXPERIMENTAL PROCEDURES

Plant Cell Culture—Arabidopsis thaliana L. (Columbia ecotype) suspension cells were grown at 24 °C under continuous light (100 μE m^{-2} s^{-1}) on a rotating table (60 rev/min) in a medium containing 20 mM KNO_3, 1.2 mM $CaCl_2$, 450 μM $MgSO_4$, 375 μM KH_2PO_4, 60 μM Na_2HPO_4, 40 μM NaH_2PO_4, 40 μM $MnSO_4$, 30 μM H_3BO_3, 25 μM glycine, 10 μM $ZnSO_4$, 5 μM Fe(III)-EDTA, 4 μM nicotinic acid, 2.5 μM pyridoxine-HCl, 1.5 μM KI, 1.2 μM thiamine-HCl, 300 nM Na_2MoO_4, 100 nM ANA, 30 nM $CoCl_2$, 30 nM $CuSO_4$, 0.1 g $liter^{-1}$ casein hydrolysate, 0.1 g $liter^{-1}$ *myo*-inositol, 15 g $liter^{-1}$ sucrose, pH 5.7. Cells were subcultured with a 1/10 dilution factor every 7 days. Experiments were carried out 1 week after subculture.

Seeds from *A. thaliana* L. (Columbia ecotype), *atnos1* (29), and *g′4-3* (30) mutants were surface-sterilized by immersion in a 4% (w/v) Bayrochlor, 50% ethanol solution for 20 min. Seeds were washed three times with ethanol and left to dry in sterile conditions. Seedlings were grown in 100 ml of half-strength Murashige and Skoog medium (Sigma), pH 5.7, supplemented with 1% sucrose, 0.5 g $liter^{-1}$ MES, and 50 μM Fe(III)-EDTA. After 1 week of culture at 24 °C under continuous light (100 μE m^{-2} s^{-1}) and shaking (60 rpm), medium was discarded and replaced by 100 ml of fresh medium. Plants were grown 4 additional days in these conditions before treatments.

Chemicals—One volume of a 100 mM $FeSO_4$ stock solution in 0.06 M HCl was mixed with 1 volume of 200 mM Na_3-citrate for a concentration of 50 mM $FeSO_4$, 100 mM Na_3-citrate. This mixture was used at final concentration of 300 μM $FeSO_4$, 600 μM Na_3-citrate in the culture medium. Except where indicated, all chemicals were purchased from Sigma. Okadaic acid and cycloheximide were dissolved in ethanol and used at final concentrations of 250 nM and 100 μM, respectively. MG132 was dissolved in Me_2SO and used at a final concentration of 50 μM. Pefabloc (Roche Applied Science), cPTIO, L-NMMA, and SNP were dissolved in sterile water and used at final concentrations of 100 μM, and 1, 5, and 2.5 mM, respectively. After treatments, cells were filtered or plantlets were collected and immediately frozen in liquid nitrogen and stored at −80 °C.

Microscopy—NO imaging was performed by using 4-amino-5-methylamino-2′,7′-difluorofluorescein diacetate (DAF-FM DA, Molecular Probes) dissolved in Me_2SO at a stock concentration of 5 mM. For confocal laser-scanning microscopy, cells were loaded with 5 μM DAF-FM DA for 20 min. Then a solution containing 300 μM $FeSO_4$, 600 μM Na_3-citrate or 300 μM K_2SO_4, 600 μM Na_3-citrate was added. The cell suspension (30 μl) was transferred on the slide. After overlaying by the glass cover, the slides were placed under the microscope, and the images were taken within 5 min on the same cells for each treatment. Settings and laser of the Zeiss Axiovert 100M inverted microscope were as described previously (31). Microscope, laser, and photomultiplier settings were held constant during the course of an experiment to obtain comparable data. Images were processed and analyzed using the Zeiss LSM 510 software.

RNA Preparation and Analysis—Total RNA were extracted from cells and plantlets as indicated in Ref. 25. For Northern blot analysis, 10 μg of total RNA were loaded in each lane, separated by electrophoresis through a 1.2% (w/v) agarose/formaldehyde gel, and blotted onto a nylon membrane (Hybond N; Amersham Biosciences). Hybridizations with ^{32}P-labeled probes were performed overnight at 42 °C in the presence of 50% formamide (32). After washes, filters were exposed for a few hours at −80 °C to Fuji Medical X-Ray film Super RX (Fujifilm) with an intensifying screen. *AtFer1* mRNA relative abundance was determined by measuring hybridization signal intensities of *AtFer1* and *EF1α* on the same blot. Quantifications were performed with the Imager Reader Bas-5000 software (Fuji). The *AtFer1* mRNA relative abundance was defined as the ratio of *AtFer1* and *EF1α* signal intensities.

Protein Preparation and Analysis—Total protein extracts were prepared from 1 g of each sample as described (33). Protein concentration was determined according to Schaffner and Weissmann (34) using bovine serum albumin as standard. Proteins were subjected to electrophoresis on a 13% polyacrylamide, 0.1% SDS gel according to Laemmli (35). After electroblotting onto Hybond-P membrane (Amersham Biosciences), immunodetection of ferritin was performed using a rabbit polyclonal antiserum raised against purified AtFer1p (24) and the Aurora Western blotting kit (ICN) following the manufacturer's recommendations.

Preparation of Nuclear Extracts—All procedures were carried out at 4 °C. Frozen cells (50 g) were ground in a Waring

Blender in 300 ml of homogenization buffer (250 mM sucrose, 10 mM NaCl, 25 mM Pipes, 5 mM EDTA, 0.15 mM spermine, 0.5 mM spermidine, 20 mM β-mercaptoethanol, 0.1% Nonidet P-40, and 0.2 mM phenylmethylsulfonyl fluoride, pH 7.0). The homogenates were filtered through two layers of Miracloth (Calbiochem). Nuclei were recovered by centrifugation at 4,200 $\times$ *g* for 20 min at 4 °C, then were gently resuspended, and washed four times with homogenization buffer with subsequent centrifugations at 2,000 $\times$ *g* for 10 min, then at 1,500 $\times$ *g* for 10, 8, and 6 min. Nuclei were resuspended in a minimum volume of freezing buffer (100 mM NaCl, 50 mM Hepes, 10 mM KCl, 5 mM $MgCl_2$, 1 mM DTT, 0.5 μg ml^{-1} leupeptin, and 50 μg ml^{-1} antipain, 50% glycerol, pH 7.6), frozen in liquid nitrogen, and stored at −80 °C until use. Nuclear extracts were prepared by thawing nuclei on ice and lysing by adjusting the NaCl concentration to 0.47 M with lysing buffer (2.5 M NaCl, 50 mM Hepes, 10 mM KCl, 5 mM $MgCl_2$, 1 mM DTT, 0.5 μg ml^{-1} leupeptin, 50 μg ml^{-1} antipain, 20% glycerol, pH 7.6), and then shaking at 4 °C for 30 min. Chromatin was pelleted by centrifugation at 13,000 $\times$ *g* for 15 min, and the supernatant containing nuclear proteins was dialyzed for 4 h against dialysis buffer (20 mM Hepes, 40 mM NaCl, 0.2 mM EDTA, 1 mM DTT, 20% glycerol, pH 7.6). Nuclear proteins were concentrated with centrifugal filter devices (Amicon, Ultracel 10k). Protein concentration was determined according to Schaffner and Weissmann (34) using bovine serum albumin as standard. Nuclear extracts were frozen in liquid nitrogen, and stored at −80 °C.

DNA Probes and Labeling Reactions—The specific probe used for *AtFer1* detection consists in a chimeric fragment containing the 5′- and 3′-untranslated regions of the *AtFer1* cDNA. The 5′-untranslated region was amplified with thermostable *Pfu* DNA polymerase (Promega) using primers 5′-GGTACCTATATA-AACCCTTCCTCCTTCC-3′ and 5′-GAATTCCATCGGCAT-GTTGTTTGTGTCC-3′ introducing KpnI and EcoRI sites at the 5′ and 3′ ends of the amplified fragment, respectively. The 3′-untranslated region was amplified using primers 5′-GAACTA-GAATTCGACCTCTATAAG-3′ and 5′-TAGAAACTAGTA-AAACAAAAACTTCATTG-3′ introducing EcoRI and SpeI sites at the 5′ and 3′ ends of the amplified fragment, respectively. The fragments were cloned at the corresponding sites in pBluescript (Stratagene) and sequenced. The specific probe (469 bp) was obtained by digesting the resulting construct by KpnI and SpeI. The *EF1α* probe (550 bp) was obtained by amplification with the *Pfu* DNA polymerase on the *EF1α* cDNA using the forward 5′-CCACCACTGGTGGTTTTGAGGCTGGTATC-3′ and reverse 5′-CATTGAACCCAACGTTGTCACCTGGAAG-3′ primers. The resulting fragment was cloned at the EcoRV site of pBluescript and sequenced. The probe was obtained after digestion of the plasmid with BamHI and HindIII. The fragments were purified on agarose gel prior to labeling. Probes were labeled with [α-^{32}P]dCTP with the use of Prime-a-Gene Labeling kit (Promega).

For the gel shift experiments, DNA probes were amplified from genomic DNA with *Pfu* DNA polymerase and different primers introducing a BamHI site at the 5′ end of the amplified fragment and a XhoI site at the 3′ end. Amplified fragments were cloned in pBluescript at the corresponding sites and sequenced. For probes A, B, C, and D (see the location of the amplified fragments on Fig. 6), the primer located at the 5′ end of the amplified fragment is 5′-GGATCCGAGCGAGTAGGA-AATA-3′. At the 3′ ends, the primers were 5′-CTCGAGAAA-GGCGTGTGGTCACCGTTGG-3′, 5′-CTCGAGCCGTTGG-ATTGAGATCC-3′, 5′-CTCGAGTGGATATGAAAGCCAG-ATGT-3′, and 5′-CTCGAGGATAGTGTGAACTGTGAG-3′ for probes A, B, C, and D, respectively. The probe E was obtained with primers 5′-GGATCCCAGATTTACACGTCT-AACTT-3′ and 5′-CTCGAGCATCTCTCCAAATAAAGTT-TGTCC-3′. For labeling and competitions, the fragments were obtained by digestion of the corresponding plasmids by BamHI and XhoI and subsequent purification on agarose gel. For labeling, 100 ng of DNA was introduced in a medium containing 50 mM Tris-HCl, pH 7.5, 10 mM $MgCl_2$, 1 mM DTT, 50 μg ml^{-1} bovine serum albumin, dATP, dGTP, dTTP (600 μM each), 50 μCi of [^{32}P]dCTP and 10 units of Klenow fragment. After 30 min at room temperature, DNA was purified by phenol/chloroform extraction and ethanol precipitation. After a 15-min centrifugation at 10,000 $\times$ *g* at 4 °C, the pellet was washed twice with 70% ethanol, dried, and re-suspended in 50 μl of water. Specific activity of the probe was determined by scintillation counting, and the probe was diluted to 20,000 cpm/μl.

Mobility Shift Assay—The mobility shift reaction was done in a volume of 30 μl using 1 μl of ^{32}P-labeled DNA fragment, 2 μg of poly(dI-dC), and 5 μg of nuclear protein in the fixation buffer (25 mM Hepes-KOH, 70 mM KCl, 1 mM EDTA, 1 mM DTT, 50% glycerol, pH 7.6). The binding reaction was performed for 30 min at room temperature prior to loading reactions onto 6% polyacrylamide non-denaturing gel in 45 mM Tris, 45 mM boric acid, 0.5 mM EDTA, 5% glycerol, pH 8.0. The gel was run at 120 V in 45 mM Tris, 45 mM boric acid, 0.5 mM EDTA, pH 8.0, buffer for ~6 h. After migration, the gel was dried during 2 h under vacuum at 80 °C and exposed for a few hours at −80 °C to Fuji Medical X-Ray film Super RX (Fujifilm). For the binding competition assays, a 50-fold molar excess of unlabeled fragments was included in the reaction.

RESULTS

Iron and H_2O_2 Increase AtFer1 mRNA Abundance by Two Independent and Additive Pathways—Both maize *ZmFer1* and *Arabidopsis AtFer1* ferritin mRNA accumulates in response to iron treatment. This response, dependent of the *cis*-acting element IDRS (18), is antagonized by antioxidants like *N*-acetylcysteine and GSH (20, 22), indicating that an oxidative step is involved in the pathway leading to the iron-dependent ferritin mRNA increase in abundance. Furthermore, it has been previously reported that H_2O_2 treatment increases maize *ZmFer1* and *Arabidopsis AtFer1* mRNA abundance (21, 22). It can therefore be hypothesized that H_2O_2 could act in the iron/IDRS-dependent pathway, and this is the first point we analyzed. We checked whether H_2O_2 treatment could mimic the potential oxidative effect of iron overload. *Arabidopsis* cell cultures were treated either with 300 μM iron-citrate, 5 mM H_2O_2, or with both inducers. Above 300 μM iron-citrate or 5 mM H_2O_2, no significant difference in *AtFer1* mRNA abundance was observed (data not shown). Cells were harvested at different time points from 1 to 48 h. Total RNA was purified and subjected to Northern analysis for determining *AtFer1* mRNA

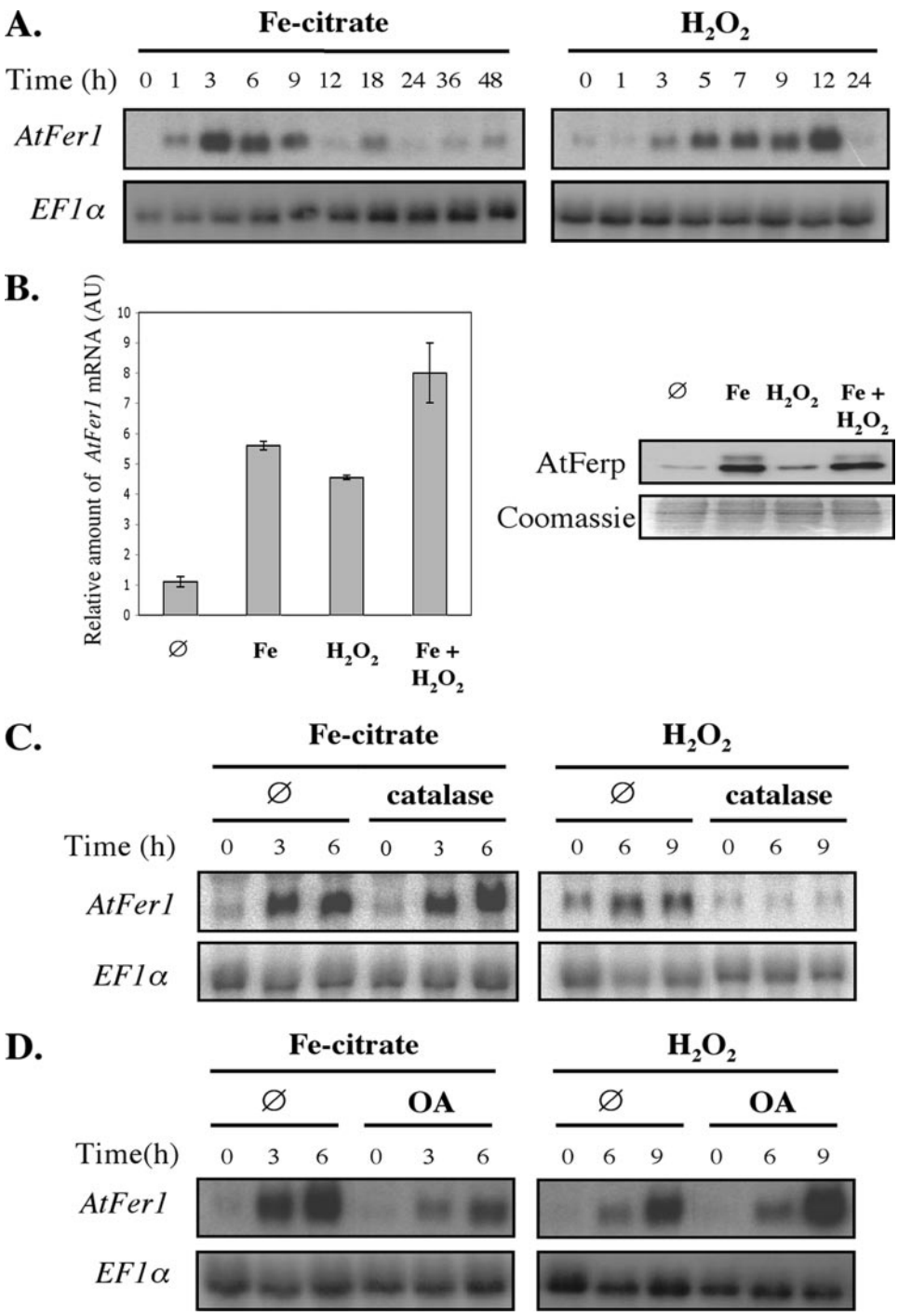

FIGURE 1. **Iron and H_2O_2 increase *AtFer1* mRNA abundance by independent pathways.** *A*, kinetic of *AtFer1* mRNA abundance in response to iron and H_2O_2 treatments. *Arabidopsis* culture cells were treated with 300 μM iron-citrate or 5 mM H_2O_2 for different times. RNA was analyzed by Northern blotting and hybridized successively with the *AtFer1* (*upper panel*) and *EF1*α (*lower panel*) probes. *EF1*α mRNA abundance was shown as loading control. *B*, effect of co-treatment with iron and H_2O_2 on mRNA and protein accumulation. For mRNA abundance determination, cells were treated for 6 h either with 5 mM H_2O_2 or 300 μM iron-citrate or co-treated with 5 mM H_2O_2, 300 μM iron-citrate. Untreated cells were used as control. Relative *AtFer1* mRNA abundance (*AtFer1*/*EF1*α signal intensities ratio) was determined from three independent experiments. *Bars* correspond to the standard deviation. For AtFer1 protein detection, cells were treated for 24 h either with 5 mM H_2O_2 or 300 μM iron-citrate or co-treated with 5 mM H_2O_2, 300 μM iron-citrate. Ten-μg protein extracts were loaded for each lane. A polyclonal serum (1/20,000 dilution) raised against AtFer1p was used for immunodetection. A Coomassie Blue-stained gel is shown as loading control. *C*, effect of catalase on the iron- and H_2O_2-mediated expression of *AtFer1*. *Arabidopsis* cells were pre-treated, when indicated, with 140 units ml^{-1} of catalase for 1 h. Either 300 μM iron-citrate or 5 mM H_2O_2 were then added to the culture medium. Cells were collected at different time points. Northern blot was performed as described above. *D*, effect of OA on the iron- and H_2O_2-mediated expression of *AtFer1*. *Arabidopsis* cells were pre-treated, where indicated, with 250 nM OA for 3 h. Either 300 μM iron-citrate or 5 mM H_2O_2 were then added to the culture medium. Cells were collected at different time points. Northern blot was performed as described in *A*.

abundance (Fig. 1*A*). In response to iron treatment, the *AtFer1* steady state mRNA level increased 1 h after iron application, reached a maximum after 3 to 6 h of treatment, and decreased. This result is in accordance with those obtained with *Arabidopsis* plantlets (20, 21). The *AtFer1* mRNA abundance was also increased after H_2O_2 treatment, but with a different time course; the maximum level of transcript was observed 12 h after H_2O_2 treatment, and *AtFer1* mRNA was barely detectable after 24 h (Fig. 1*A*). *AtFer1* mRNA abundance after co-treatment with both effectors was compared with the effect of iron or H_2O_2 applied alone. *AtFer1* mRNA abundance was normalized relatively to the *EF1*α mRNA abundance. As shown on Fig. 1*B*, the addition of both effectors led to a signal intensity quite close to the sum of the values obtained with iron or H_2O_2 applied alone. This result indicates that iron and H_2O_2 are acting in two independent and additive pathways leading to *AtFer1* mRNA accumulation. However, addition of iron could cause the production of a certain amount of H_2O_2, potentially leading to a further *AtFer1* mRNA accumulation. Such an hypothesis is unlikely because when cells were treated with catalase prior to iron addition, no change in *AtFer1* mRNA accumulation was observed compared with catalase untreated cells (Fig. 1*C*). At the protein level, ferritin was accumulated after 24 h of iron treatment. It was also accumulated at the same time point after H_2O_2 treatment, but to a lower extend. Co-treatment with iron and H_2O_2 led to a ferritin protein accumulation to a level close to the one that was observed in response to iron treatment (Fig. 1*B*). Moreover, we have tested the effect of okadaic acid (OA) on *AtFer1* mRNA abundance in response to iron excess or H_2O_2 treatments. It has to be reminded that OA has been shown to antagonize maize *ZmFer1* gene expression both in response to iron excess and H_2O_2 treatment. When *Arabidopsis*

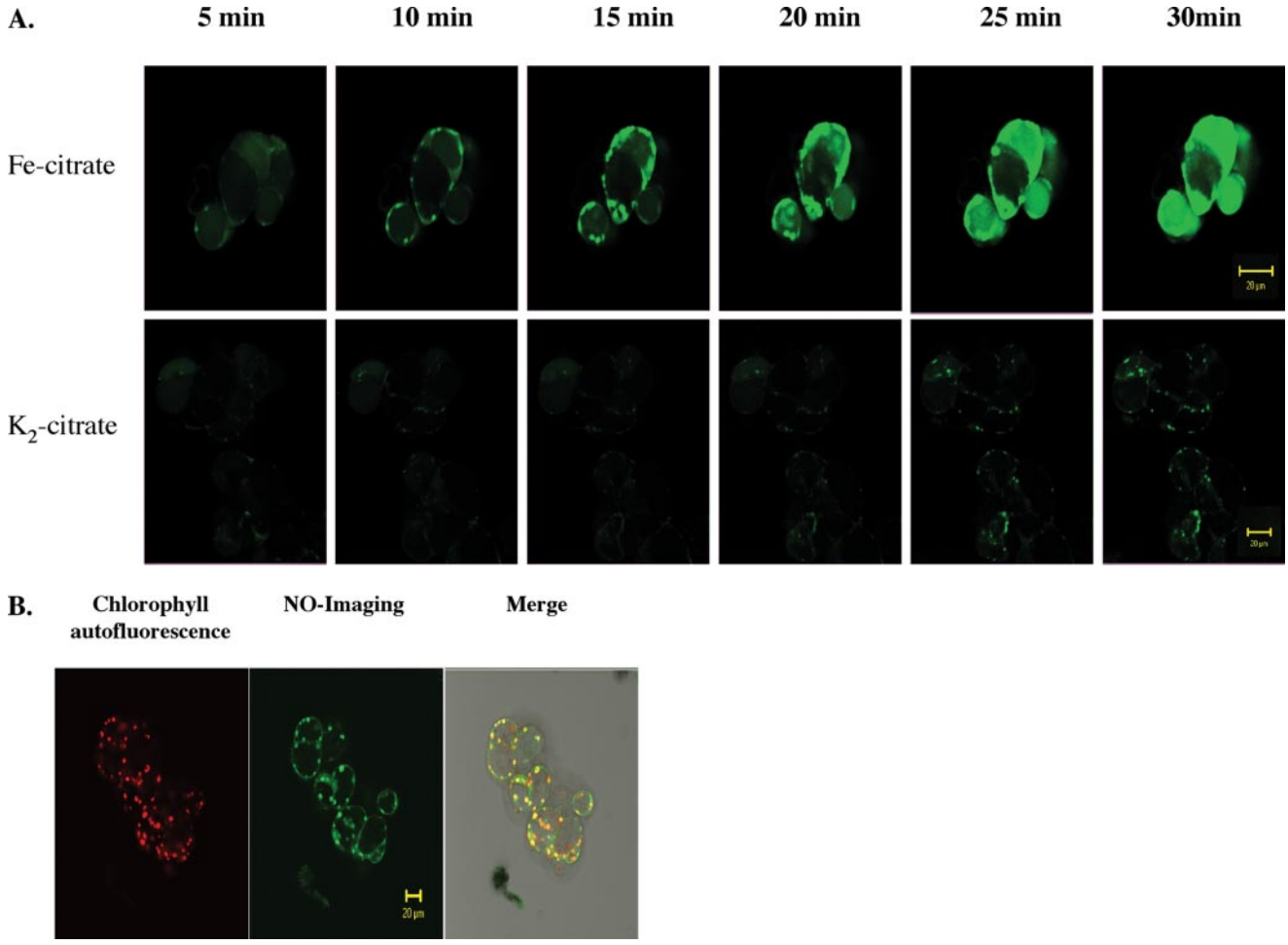

FIGURE 2. **Iron treatment leads to a plastid-located NO burst.** *A*, kinetic of NO accumulation in iron-treated cells. Cells were loaded with DAF-FM DA for 30 min, and 300 μM iron-citrate or 300 μM K_2-citrate was added. The fluorescence of DAF-FM DA (excitation 495 nm, emission 515 nm) was visualized by confocal laser scanning after effector addition at different time points. *B*, localization of NO production in plastids. In the same cells, chlorophyll autofluorescence and DAF-FM DA were visualized, and the two images were superimposed.

cells were treated with OA, iron-induced *AtFer1* mRNA abundance was decreased, whereas H_2O_2-induced mRNA abundance was increased (Fig. 1*D*). This indicates that a PP2A-type phosphatase is a positive regulator of the iron pathway and a negative regulator of the H_2O_2 pathway. This result enforces the hypothesis of independent pathways. Although we cannot rule out that reactive oxygen species other than H_2O_2 could be involved in the increase of *AtFer1* mRNA abundance, it is more likely that the response is specific to H_2O_2 because catalase addition prior to H_2O_2 treatment abolished *AtFer1* mRNA accumulation (Fig. 1*C*). Our main goal being to decipher the iron- and IDRS-dependent pathway, we further investigate only the response of *AtFer1* gene to iron treatment.

An Iron-induced Plastidial NO Burst Precedes AtFer1 mRNA Accumulation—Several reports have involved nitric oxide in the control of iron homeostasis and in *AtFer1* regulation (26, 27, 36–38). NO was shown to be involved in iron- and IDRS-dependent *AtFer1* regulation (26, 27). SNP (a NO donor) induced an *AtFer1* mRNA abundance increase and cPTIO (a NO scavenger) antagonized iron-induced *AtFer1* mRNA accumulation. We have first examined whether iron treatment may lead to a NO production in the cells by using the NO-sensitive fluorescent probe DAF-FM DA. Cells were incubated for 20 min with the probe before the application of treatments. NO production was visualized using a confocal microscope (Fig. 2). The iron-citrate treatment led to a very rapid increase of the fluorescence. A clear signal was detected 5 min after iron-citrate addition. Its intensity increased and reached a maximum after 30 min (Fig. 2*A*). A control treatment made with potassium replacing iron as cation did not lead to such a strong fluorescence increase, indicating that the NO production observed was specific of iron. Furthermore, the DAF-FM DA fluorescence pattern observed at the early times of the kinetic merged with the red chlorophyll autofluorescence (Fig. 2*B*). This indicates that iron treatment leads to a rapid NO burst in the plastids. After 30 min of iron treatment, the fluorescence was very intense and was also detected in both the nucleus and the cytosol of the cells.

The next step was to examine further the origin of the NO production regulating *AtFer1* expression. Cells were treated with animal NO synthase inhibitors prior to iron addition. A treatment with L-NMMA decreased *AtFer1* mRNA abundance in response to iron treatment (Fig. 3*A*). The same decrease was obtained with N^{ω}-nitro-L-arginine methyl ester (data not shown). We used both SNP and cPTIO as controls, and, as previously reported (26, 27), these compounds increased and

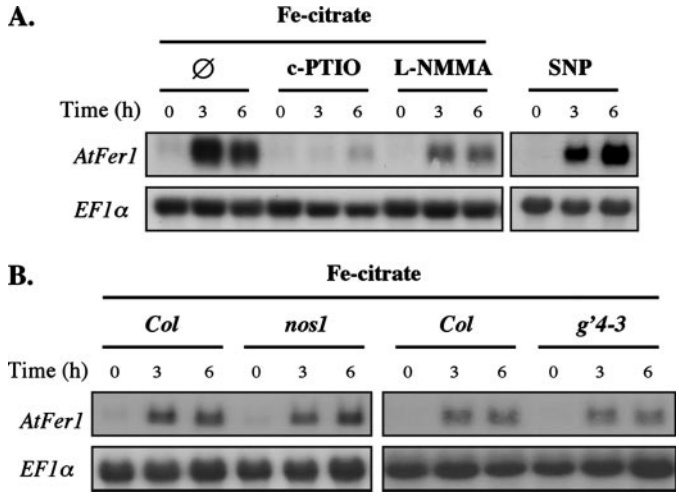

FIGURE 3. **Implication of nitric oxide on iron-mediated *AtFer1* expression.** *A*, effect of NO scavenger, NO donor, and NOS inhibitors. Cells were pre-treated for 1 h with 1 mM cPTIO or 5 mM L-NMMA prior to 300 μM iron-citrate addition. SNP (2.5 mM) was added without iron. Cells were collected at different time points. Northern blot analysis was performed as described in the legend to Fig. 1. *B*, implication of NR and NOS1 in *AtFer1* iron-mediated expression. Ten-day-old wild-type *Arabidopsis* (*Columbia* ecotype), *nos1* and *g'4-3* mutants plantlets, cultivated *in vitro*, were treated, where indicated, with 300 μM iron-citrate for 3 and 6 h. RNA extracted from plantlets were analyzed by Northern blotting and hybridized successively with *AtFer1* and *EF1α* probes.

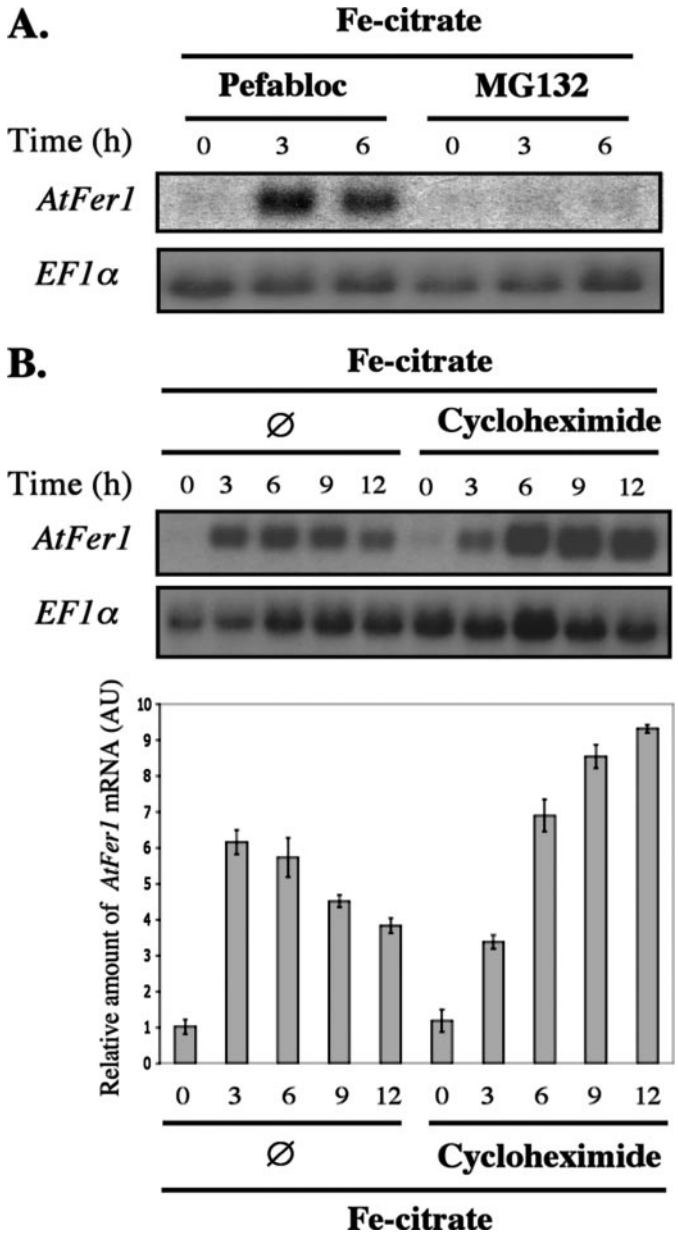

FIGURE 4. **Effect of protein degradation and synthesis inhibitors on the iron-mediated expression of *AtFer1*.** *A*, effect of protein degradation inhibitors. Cells were pretreated for 1 h with 100 μM Pefabloc or 50 μM MG132, then 300 μM $FeSO_4$, 600 μM Na_3-citrate was added in culture medium. Cells were collected before, and 3 and 6 h after iron treatment. Northern blot was performed as described in the legend to Fig. 1. *B*, effect of cycloheximide. Cells were pre-treated, where indicated, with 100 μM cycloheximide for 1 h prior the addition of 300 μM iron-citrate. Samples were collected at different time points, and *AtFer1* mRNA abundance was examined as before. *AtFer1* mRNA relative abundance was determined as described in the legend to Fig. 1. *Bars* correspond to the standard deviation from three independent experiments.

decreased, respectively, *AtFer1* mRNA abundance (Fig. 3*A*). The decrease observed with L-NMMA treatment suggests that a NO synthase activity could be required for the iron-dependent *AtFer1* up-regulation. So far, two enzymes have been implicated in NO production in plants (39, 40): the nitrate reductase and the NO synthase NOS1. To determine whether these enzymes are involved in NO production leading to *AtFer1* mRNA accumulation in response to iron excess, the loss of function mutants *g'4-3* (30) and *atnos1* (29) were used. The *g'4-3* mutant is deficient in both *nia1* and *nia2* gene activities and displays only 0.5% of the wild-type shoot nitrate reductase (NR) activity. *Arabidopsis* cell lines of these two mutants are not available. Therefore, experiments were performed on plantlets grown under sterile conditions. In this plantlet system, *AtFer1* response to iron treatment is not altered (20), and NO treatment led to an increase of *AtFer1* mRNA abundance, in the same manner as in the cell culture system (data not shown). In the two mutants, the abundance of *AtFer1* mRNA after iron application was similar to the one observed in wild-type plants (Fig. 3*B*). These results indicate that neither nitrate reductase nor NOS1 are involved in iron-dependent NO production leading to *AtFer1* regulation.

AtFer1 Repressor Is Degraded by a 26 S Proteasome-dependent Pathway—The *cis*-acting element IDRS has been shown to be involved in iron-dependent *AtFer1* de-repression (18). This suggests that a repressor acts in the pathway, and that iron addition leads to a de-repression of *AtFer1* transcription, rather than to activation (18, 27). This also suggests that iron treatment may lead to the inactivation or the degradation of a repressor. To test this latter hypothesis, and more specifically the involvement of a 26 S proteasome-dependent protein degradation, we used the specific 26 S proteasome inhibitor MG132. Cells were treated with MG132 prior to iron treatment. A general serine protease inhibitor, Pefabloc, was used in the same conditions as a control (Fig. 4*A*). Pefabloc did not affect the iron-dependent *AtFer1* regulation, whereas MG132 treatment completely abolished the response. This result indicates that a protein, involved in the repression of *AtFer1* transcription in low iron conditions, is ubiquitinated and degraded by a 26 S proteasome-dependent pathway after iron treatment. This factor was named repressor.

As protein degradation appears to be involved in *AtFer1* de-repression, we have also checked whether protein synthesis

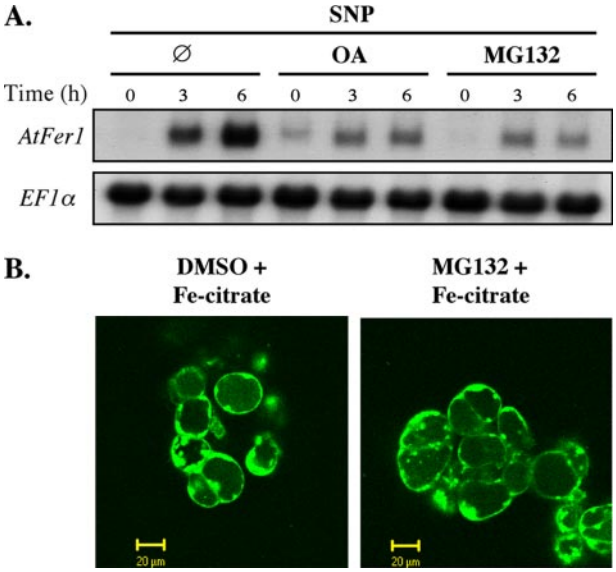

FIGURE 5. **Order of the molecular events in iron-mediated *AtFer1* expression signaling pathway.** *A*, effect of co-treatments on *AtFer1* mRNA abundance. Cells were pre-treated, where indicated, with 250 nM OA or 50 μM MG132 for 3 and 1 h, respectively. Then, SNP (2.5 mM final concentration) was added into medium culture, and cells were collected 1 h later. Northern blot was performed as described in the legend to Fig. 1. *B*, effect of MG132 on the iron-mediated NO burst. Cells were loaded with DAF-FM DA for 30 min, and MG132 (final concentration 50 μM) or Me_2SO (*DMSO*) (control) were added. Cells were incubated for 15 min. The fluorescence of DAF-FM DA (excitation 495 nm, emission 515 nm) was visualized by confocal laser scanning 20 min after iron-citrate addition.

may arise in the pathway. Cells were treated with cycloheximide prior to iron addition, and harvested at different time points from 3 to 12 h. A control kinetic was performed with untreated cells. As shown on Fig. 4*B*, 3 h after the iron addition, *AtFer1* mRNA abundance was not affected by the cycloheximide. By contrast, after 6 h and later, mRNA abundance was increased by cycloheximide treatment. The decrease of mRNA abundance observed 9 and 12 h after iron treatment was greatly reduced by addition of cycloheximide. This suggests that *de novo* synthesis of the repressor, and/or of protein(s) involved in the *AtFer1* mRNA turnover, is necessary to decrease ferritin mRNA abundance in the latter times of the kinetic after iron addition.

So far, three elements have been identified in the signal transduction pathway leading to the *AtFer1* response to iron. Two positive regulators of the mRNA accumulation: NO and a PP2A-type phosphatase, and a negative regulator: the repressor. To position them with respect to the others in the pathway, cells were co-treated with two effectors at the same time. We used SNP, which promotes an *AtFer1* mRNA increase in abundance, and OA and MG132, which leads to a decrease of the transcript level. The positive effect of SNP treatment on the *AtFer1* mRNA level was abolished by both OA and MG132 treatments (Fig. 5*A*). Therefore, NO production by SNP cannot bypass the effect of the two inhibitors, MG132 and OA. This indicates that NO production, acting downstream of iron, could act upstream of the PP2A-type phosphatase and the repressor. However, because all protein degradation (*i.e.* not only the repressor) by the 26 S proteasome is blocked by MG132, it is possible that protein degradation acts further upstream in the pathway. It can be hypothesized that degradation of some proteins could be required for NO production. Thus, altering the NO production by MG132 could also explain why *AtFer1* mRNA does not accumulate in response to treatment with this proteasome inhibitor. To show that NO generation in response to iron treatment occurs independently of the proteasome, *Arabidopsis* cells were treated with iron and MG132, and NO production was monitored by DAF imaging. The fluorescence observed was similar to the one of control cells treated with iron in the absence of MG132, showing that iron-dependent NO production was not altered by MG132 (Fig. 5*B*).

AtFer1 Repressor Is Not Bound to the IDRS—As the IDRS *cis*-acting element has been shown to be involved in *AtFer1* de-repression, it was tempting to postulate that the repressor could be a transcription factor bound to the IDRS in low iron conditions, and degraded upon iron addition. To test this hypothesis, we first checked whether the *AtFer1* IDRS could bind nuclear factors. Nuclear extracts were prepared from untreated cells and from cells treated with iron (de-repression condition), or with MG132 (repression condition). A ^{32}P radiolabeled DNA probe corresponding to a 200-bp region of the *AtFer1* promoter sequence, and containing the IDRS (probe A; Fig. 6*A*), was incubated with nuclear proteins. Only one complex was observed by gel shift (Fig. 6*B*). To check the specificity of this complex, the binding reaction was performed with a 50-fold molar excess of different unlabeled DNA fragments. With DNA fragments containing the IDRS (probes A, B, and C, Fig. 6*A*), the signal corresponding to the complex was completely abolished, whereas it was not modified with probes that did not contain the IDRS sequence (probes D and E, Fig. 6*A*). Results indicate that the complex observed consists of nuclear proteins bound to the IDRS. The intensity of the DNA-protein(s) complex signal was almost the same with extracts prepared from untreated, iron-treated, and MG132-treated cells (Fig. 6*B*), suggesting that complex formation is the same under repressive and de-repressive conditions. Taken together, results suggest that a repressor is acting upstream of the nuclear protein(s), which are stably bound to the IDRS, both in repressive or in de-repressive conditions. Such repressor is degraded by the proteasome in de-repressive conditions.

DISCUSSION

Our current knowledge on ferritin gene expression in plants is largely based on work on maize *ZmFer* genes (18, 19, 22, 25) and on the *Arabidopsis AtFer1* gene (20, 21, 23, 27, 28). We used an *Arabidopsis* cell culture system to further characterize the pathway leading to *AtFer1* de-repression after iron addition.

The *AtFer1* mRNA level is enhanced by both iron and H_2O_2 treatments (Fig. 1*A*). This result is consistent with the studies on the maize *ZmFer1* gene, which is orthologous to *AtFer1* (22). As a highly reactive transition metal, iron may lead to oxidative stress. By sequestering free iron, the accumulation of ferritin may prevent oxidative damage. In maize, *ZmFer1* mRNA abundance in response to iron treatment is antagonized by antioxidants like *N*-acetylcysteine and GSH, indicating that the iron effect on ferritin mRNA abundance is dependent of an oxidative step (22). Both iron- and H_2O_2-dependent *ZmFer1* mRNA

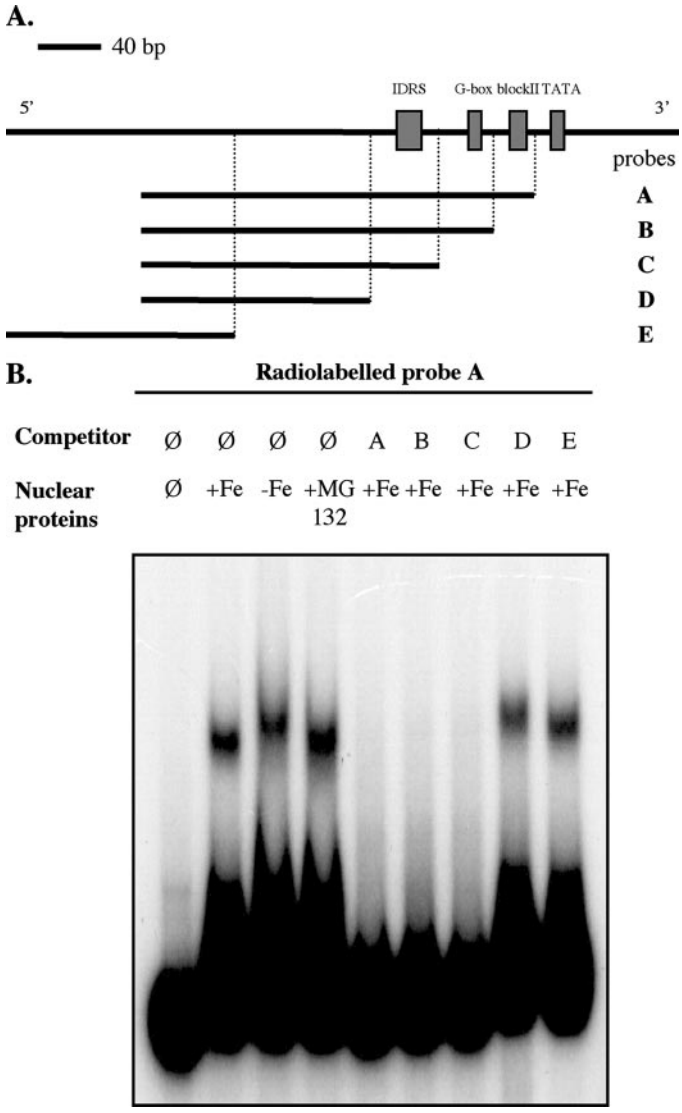

FIGURE 6. **Specific binding of *Arabidopsis* nuclear protein(s) to the IDRS.** *A*, localization of the DNA probes used for the gel shift experiments on *AtFer1* promoter region. The putative regulatory elements indicated by *boxes* are those defined by Petit *et al.* (18). *TATA*, TATA box. *B*, mobility shift assays. Five μg of nuclear protein extracts from *Arabidopsis* cells untreated (−*Fe*), or treated for 3 h either with 300 μM iron-citrate (+*Fe*) or 1 h with 50 μM MG132 (+*MG132*) were incubated for 30 min at room temperature with radiolabeled probe A. For the competition assays, a 50-fold molar excess of unlabeled fragments was added in the reaction.

regulation are sensitive to okadaic acid. This is consistent with the hypothesis that these inducers could act through the same oxidative pathway leading to an increased *ZmFer1* mRNA abundance (22). In contrast to *ZmFer1*, OA strongly decreased *AtFer1* mRNA abundance in response to iron (Fig. 1*D*). Furthermore, the amount of the *AtFer1* transcript in response to H_2O_2 is increased after okadaic acid treatment. Thus, a PP2A-type phosphatase may be an activator of the iron-dependent pathway, and a repressor of the H_2O_2-dependent pathway. The two pathways appear therefore totally independent. This is in full agreement with the observation that the abundance of the *AtFer1* mRNA in response to the addition of the two effectors at the same time is closed to the sum of the transcript abundance observed in response to each effector when applied alone (Fig. 1*B*). However, the iron-dependent *AtFer1* mRNA increase in abundance has been previously shown to be antagonized by *N*-acetylcysteine treatment, revealing the involvement of an oxidative step in this response (20). This suggests that two different oxidative signals are involved in both iron- and H_2O_2-dependent pathways. At the protein level, we observed a higher amount of ferritin accumulated in response to iron treatment than in response to H_2O_2 treatment (Fig. 1*B*). This is consistent with previous data indicating that iron is required for ferritin protein stabilization (25).

In the present work, we have shown that iron addition leads to NO accumulation in the plastids (Fig. 2). NO is an essential growth regulator in plants, and serves as a signal in biotic and abiotic stress responses, programmed cell death, hormone responses, root and xylem development, flowering, and iron homeostasis (reviewed in Refs. 37 and 39–45). The inhibitory effect of L-NMMA on *AtFer1* expression in response to iron excess indicates that NO synthase activity is involved in the pathway (Fig. 3). In plant cells, the two enzymes so far reported to be implicated in NO synthesis are the NR and a nitric-oxide synthase (NOS1). NR is a cytosolic located enzyme, and NOS1 has recently been shown to be targeted to the mitochondria (46). Thus, none of these enzymes could produce NO in the plastids. Such a conclusion is consistent with the observation that *AtFer1* expression in response to iron is not altered in the mutants *g′4-3* and *atnos1* (Fig. 3). Although there is so far no conclusive evidence for enzymatic NO production in the plastids, there are two indirect observations in favor of this hypothesis. First, an immunoreactive NOS protein has been detected in plastids (47). Second, the addition of the plant defense elicitor cryptogein on epidermal tobacco cells leads to a N^{ω}-nitro-L-arginine methyl ester-sensitive NO production in the plastid (48, 49). These results indicate that NO synthase activity is probably present in the plastid, but the nature of the enzyme involved remains to be determined.

A NO scavenger, cPTIO, completely abolishes iron-dependent *AtFer1* expression, clearly establishing that NO is a major element in this signal transduction pathway. In contrast to cPTIO, L-NMMA application decreases *AtFer1* response by only 50% when compared with untreated cells (based on relative *AtFer1* mRNA abundance compared with *EF1α*; data not shown). Such a partial inhibition could be attributed to an incomplete action of this inhibitory compound. However, it cannot be excluded that both an enzymatic and a non-enzymatic (insensitive to the inhibitor used) pathway may lead to NO production in response to iron. Indeed, it is known that in plants, non-enzymatic NO production can arise from reactions between nitrite and various plant metabolites (50–52). Such a non-enzymatic NO production from nitrite has in particular been reported to occur at acidic pH in the apoplasm for example (52) and could explain the NO effects on germinating seeds (52–54). However, such a nitrite-dependent NO production is unlikely to occur in the stroma of plastids where the pH value is 7.0 or higher (55, 56).

Regardless the origin of the NO produced in the plastid in response to iron, this NO burst is an early event in the signal transduction pathway. This suggests that a retrograde signal, of unknown nature, could be produced in the plastid and lead to

the transcription of the nuclear-encoded *AtFer1* gene. Two major future prospects arise from this work and concern the identification of the site of action of NO in the pathway, and the nature of the retrograde signal. In animals, it is documented that the redox-related species of NO can have simultaneous effects on cellular iron metabolism and homeostasis via mechanisms that might involve *S*-nitrosylation (57), ligation of NO to iron-sulfur clusters (58, 59) or to heme-containing proteins (60, 61). NO and free iron may also form complexes with low molecular weight thiols like glutathione and cysteine (62–64). These dinitrosyl-iron complexes are relatively stable in contrast to the highly reactive free NO molecule (65, 66) and were shown to be potential NO carrier molecules in mammals (62). In plants, interactions of NO with hemes (67–69) or iron-sulfur clusters (70), and *S*-nitrosylation reactions (71) have been shown, and dinitrosyl-iron complexes have been detected (72). A post-translational modification of a plastidial protein by NO could be involved in the pathway leading to *AtFer1* de-repression. Alternatively, a dinitrosyl-iron complex with glutathione, which has been shown to permeate quickly through membranes (73), could be a good candidate for a retrograde signal.

Plant ferritin mRNA accumulation can be promoted by ABA (25), H_2O_2 (Refs. 21 and 22, this work), and NO (Ref. 27, this work). Whether or not these inducers act in the same pathway has not been documented. Interestingly, by combining pharmacological, biochemical, and genetic approaches, it has recently been demonstrated that ABA-induced NO production via NR is required for ABA-induced H_2O_2-mediated stomatal closure (74). It is, however, unlikely that such a pathway occurs in the regulation of *AtFer1* gene expression for the following reasons. First, we show that NO production in response to iron treatment is not mediated by NR (Fig. 3*B*). Second, among the ferritin gene families, only *AtFer2* in *Arabidopsis* and *ZmFer2* in maize have been reported to be regulated by ABA (19, 21). The *AtFer1* gene is not regulated by ABA, and the ABA-regulated *AtFer2* gene is not modulated by H_2O_2 (21).

A growing number of reports involve ubiquitination of positive or negative regulatory proteins, and their subsequent 26 S proteasome-dependent degradation as key steps of control within signaling pathways (75–77). Protein ubiquitination and subsequent degradation have been involved in light, auxin, ethylene, pathogen resistance, and more recently in phosphate starvation responses (78). The presence of a repressor in iron-mediated *AtFer1* regulation of expression prompted us to examine whether inhibitors of the proteasome-dependent protein degradation could alter the iron response or not. Indeed, the use of MG132 dramatically decreases *AtFer1* mRNA abundance. This result indicates that a protein acting in low iron conditions, called the repressor, is ubiquitinated after iron addition and subsequently degraded by the 26 S proteasome. This iron-triggered degradation leads to a de-repression of *AtFer1* transcription and to the increase in abundance of the corresponding mRNA. Protein synthesis inhibition by cycloheximide perturbs such an increase, because at later time points of the kinetic (from 6 to 12 h) protein synthesis inhibition leads to a higher increased abundance of the *AtFer1* mRNA compared with control cells untreated with cycloheximide (Fig. 4*B*). Therefore, it can be proposed that *de novo* synthesis of the repressor is necessary to decrease *AtFer1* mRNA abundance about 6–9 h after iron addition. In fact, such a cycloheximide-promoted superinduction has been largely documented and can be attributed not only to a transcriptional de-repression (79, 80) but also to a decrease of mRNA degradation (79–82). Our results cannot discriminate between these two possibilities.

Mutagenesis of the IDRS *cis*-element within the maize *ZmFer1* or *Arabidopsis AtFer1* promoter sequences leads to de-repression of the expression of reporter genes, in the absence of iron treatment (18). It can be therefore hypothesized that the repressor could bind to the IDRS in low iron conditions and that iron treatment would promote its ubiquitination and degradation, resulting in *AtFer1* gene expression. MG132 treatment of the cells would avoid the repressor degradation, maintain its binding to the IDRS and repress *AtFer1* gene expression, even after iron treatment. However, nuclear protein(s) from cells either treated with iron or MG132, or untreated bind equally to the IDRS, without significant difference in size or intensity of the complex formed (Fig. 6). Therefore, the protein ubiquitinated and degraded in response to iron treatment, and defined as the repressor, is unlikely to be a *trans*-acting factor able to directly bind to the IDRS in low iron conditions. This result is consistent with the observation that no significant difference in the intensity of the *ZmFer1* IDRS-protein complex was observed by gel shift experiments using nuclear extracts of iron-treated or untreated maize plants (18). Thus, it is proposed that the transcription factor(s) bound to the IDRS is(are) essential but not sufficient for *AtFer1* de-repression, and that the repressor acts upstream of this transcription factor.

It is worth noticing that in animal cells, one of the ferritin *trans* regulators involved in the translational repression of ferritin mRNAs in low iron conditions, namely IRP2, is regulated by NO and ubiquitin. After iron addition, IRP2 has been shown to be nitrosylated and subsequently ubiquitinated, and degraded by the proteasome, thus leading to ferritin mRNA translation (14, 15). Our work shows that NO and protein degradation via proteasome are also involved in the regulation of ferritin gene expression in plants. It is remarkable that molecular effectors of the response to iron excess, such as NO and ubiquitination, are conserved between the translational regulation of animal ferritin and the transcriptional regulation of plant ferritin.

Acknowledgments—We thank Dr. Nigel Crawford for providing the atnos1 mutant seeds. We thank Drs. Geneviève Conejero and Gaëlle Viennois for expertise in confocal microscopy. We thank Gabriel Krouk, Karl Ravet, and Drs. Alain Pugin and Thierry Lagrange for helpful discussions.

REFERENCES

1. Guerinot, M. L., and Yi, Y. (1994) *Plant Physiol.* **104,** 815–820
2. Noctor, G., and Foyer, C. H. (1998) *Annu. Rev. Plant Physiol. Plant Mol. Biol.* **49,** 249–279
3. Harrison, P. M., and Arosio, P. (1996) *Biochim. Biophys. Acta* **1275,** 161–203
4. Hentze, M. W., and Kuhn, L. C. (1996) *Proc. Natl. Acad. Sci. U. S. A.* **93,** 8175–8182

5. Iwai, K., Klausner, R. D., and Rouault, T. A. (1995) *EMBO J.* **14,** 5350–5357
6. Guo, B., Phillips, J. D., Yu, Y., and Leibold, E. A. (1995) *J. Biol. Chem.* **270,** 21645–21651
7. Pantopoulos, K. (2004) *Ann. N. Y. Acad. Sci.* **1012,** 1–13
8. Kim, S., and Ponka, P. (2003) *Biometals* **16,** 125–135
9. Gardner, P. R., Costantino, G., Szabo, C., and Salzman, A. L. (1997) *J. Biol. Chem.* **272,** 25071–25076
10. Pantopoulos, K., and Hentze, M. W. (1995) *Proc. Natl. Acad. Sci. U. S. A.* **92,** 1267–1271
11. Kim, S., and Ponka, P. (2000) *J. Biol. Chem.* **275,** 6220–6226
12. Bouton, C., Oliveira, L., and Drapier, J. C. (1998) *J. Biol. Chem.* **273,** 9403–9408
13. Kim, S., and Ponka, P. (1999) *J. Biol. Chem.* **274,** 33035–33042
14. Kim, S., and Ponka, P. (2002) *Proc. Natl. Acad. Sci. U. S. A.* **99,** 12214–12219
15. Kim, S., Wing, S. S., and Ponka, P. (2004) *Mol. Cell. Biol.* **24,** 330–337
16. Zancani, M., Peresson, C., Biroccio, A., Federici, G., Urbani, A., Murgia, I., Soave, C., Micali, F., Vianello, A., and Macri, F. (2004) *Eur. J. Biochem.* **271,** 3657–3664
17. Lescure, A. M., Proudhon, D., Pesey, H., Ragland, M., Theil, E. C., and Briat, J. F. (1991) *Proc. Natl. Acad. Sci. U. S. A.* **88,** 8222–8226
18. Petit, J. M., van Wuytswinkel, O., Briat, J. F., and Lobréaux, S. (2001) *J. Biol. Chem.* **276,** 5584–5590
19. Fobis-Loisy, I., Loridon, K., Lobréaux, S., Lebrun, M., and Briat, J. F. (1995) *Eur. J. Biochem.* **231,** 609–619
20. Gaymard, F., Boucherez, J., and Briat, J. F. (1996) *Biochem. J.* **318,** 67–73
21. Petit, J. M., Briat, J. F., and Lobréaux, S. (2001) *Biochem. J.* **359,** 575–582
22. Savino, G., Briat, J. F., and Lobréaux, S. (1997) *J. Biol. Chem.* **272,** 33319–33326
23. Murgia, I., Briat, J. F., Tarantino, D., and Soave, C. (2001) *Plant Physiol. Biochem.* **39,** 1–10
24. Dellagi, A., Rigault, M., Segond, D., Roux, C., Kraepiel, Y., Cellier, F., Briat, J. F., Gaymard, F., and Expert, D. (2005) *Plant J.* **43,** 262–272
25. Lobréaux, S., Hardy, T., and Briat, J. F. (1993) *EMBO J.* **12,** 651–657
26. Murgia, I., de Pinto, M. C., Delledonne, M., Soave, C., and De Gara, L. (2004) *J. Plant Physiol.* **161,** 777–783
27. Murgia, I., Delledonne, M., and Soave, C. (2002) *Plant J.* **30,** 521–528
28. Tarantino, D., Petit, J. M., Lobréaux, S., Briat, J. F., Soave, C., and Murgia, I. (2003) *Planta* **217,** 709–716
29. Guo, F. Q., Okamoto, M., and Crawford, N. M. (2003) *Science* **302,** 100–103
30. Wilkinson, J. Q., and Crawford, N. M. (1993) *Mol. Gen. Genet.* **239,** 289–297
31. Huang, X., Stettmaier, K., Michel, C., Hutzler, P., Mueller, M. J., and Durner, J. (2004) *Planta* **218,** 938–946
32. Rosen, K. M., Lamperti, E. D., and Villa-Komaroff, L. (1990) *BioTechniques* **8,** 398–403
33. Lobréaux, S., Massenet, O., and Briat, J. F. (1992) *Plant Mol. Biol.* **19,** 563–575
34. Schaffner, W., and Weissmann, C. (1973) *Anal. Biochem.* **56,** 502–514
35. Laemmli, U. K. (1970) *Nature* **227,** 680–685
36. Graziano, M., and Lamattina, L. (2005) *Trends Plant Sci.* **10,** 4–8
37. Lamattina, L., Garcia-Mata, C., Graziano, M., and Pagnussat, G. (2003) *Annu. Rev. Plant Physiol. Plant Mol. Biol.* **54,** 109–136
38. Graziano, M., Beligni, M. V., and Lamattina, L. (2002) *Plant Physiol.* **130,** 1852–1859
39. Crawford, N. M., and Guo, F. Q. (2005) *Trends Plant Sci.* **10,** 195–200
40. Crawford, N. M. (2006) *J. Exp. Bot.* **57,** 471–478
41. Delledonne, M. (2005) *Curr. Opin. Plant Biol.* **8,** 390–396
42. Lamotte, O., Courtois, C., Barnavon, L., Pugin, A., and Wendehenne, D. (2005) *Planta* **221,** 1–4
43. Neill, S. J., Desikan, R., and Hancock, J. T. (2003) *New Phytol.* **159,** 11–35
44. Wendehenne, D., Durner, J., and Klessig, D. F. (2004) *Curr. Opin. Plant Biol.* **7,** 449–455
45. Wendehenne, D., Pugin, A., Klessig, D. F., and Durner, J. (2001) *Trends Plant Sci.* **6,** 177–183
46. Guo, F. Q., and Crawford, N. M. (2005) *Plant Cell* **17,** 3436–3450
47. Barroso, J. B., Corpas, F. J., Carreras, A., Sandalio, L. M., Valderrama, R., Palma, J. M., Lupianez, J. A., and del Rio, L. A. (1999) *J. Biol. Chem.* **274,** 36729–36733
48. Foissner, I., Wendehenne, D., Langebartels, C., and Durner, J. (2000) *Plant J.* **23,** 817–824
49. Gould, K. S., Lamotte, O., Klinguer, A., Pugin, A., and Wendehenne, D. (2003) *Plant Cell Environ.* **26,** 1851–1862
50. Klepper, L. A. (1990) *Plant Physiol.* **93,** 26–32
51. Nishimura, H., Hayamizu, T., and Yanagisawa, S. (1986) *Environ. Sci. Technol.* **20,** 413–416
52. Bethke, P. C., Badger, M. R., and Jones, R. L. (2004) *Plant Cell* **16,** 332–341
53. Beligni, M. V., and Lamattina, L. (2000) *Planta* **210,** 215–221
54. Bethke, P. C., Gubler, F., Jacobsen, J. V., and Jones, R. L. (2004) *Planta* **219,** 847–855
55. Hauser, M., Eichelmann, H., Oja, V., Heber, U., and Laisk, A. (1995) *Plant Physiol.* **108,** 1059–1066
56. Song, C. P., Guo, Y., Qiu, Q., Lambert, G., Galbraith, D. W., Jagendorf, A., and Zhu, J. K. (2004) *Proc. Natl. Acad. Sci. U. S. A.* **101,** 10211–10216
57. Hess, D. T., Matsumoto, A., Kim, S. O., Marshall, H. E., and Stamler, J. S. (2005) *Nat. Rev. Mol. Cell Biol.* **6,** 150–166
58. Drapier, J. C. (1997) *Methods* **11,** 319–329
59. Richardson, D. R., Neumannova, V., and Ponka, P. (1995) *Biochim. Biophys. Acta* **1266,** 250–260
60. Joshi, M. S., Ferguson, T. B., Jr., Han, T. H., Hyduke, D. R., Liao, J. C., Rassaf, T., Bryan, N., Feelisch, M., and Lancaster, J. R., Jr. (2002) *Proc. Natl. Acad. Sci. U. S. A.* **99,** 10341–10346
61. Ishikawa, H., Kato, M., Hori, H., Ishimori, K., Kirisako, T., Tokunaga, F., and Iwai, K. (2005) *Mol. Cell* **19,** 171–181
62. Mulsch, A., Mordvintcev, P. I., Vanin, A. F., and Busse, R. (1993) *Biochem. Biophys. Res. Commun.* **196,** 1303–1308
63. Severina, I. S., Bussygina, O. G., Pyatakova, N. V., Malenkova, I. V., and Vanin, A. F. (2003) *Nitric Oxide* **8,** 155–163
64. Stamler, J. S., Singel, D. J., and Loscalzo, J. (1992) *Science* **258,** 1898–1902
65. Vanin, A. F. (1995) *Biochemistry* **60,** 225–230
66. Vanin, A. F., Stukan, R. A., and Manukhina, E. B. (1996) *Biochim. Biophys. Acta* **1295,** 5–12
67. Dordas, C., Rivoal, J., and Hill, R. D. (2003) *Ann. Bot.* **91,** 173–178
68. Millar, A. H., and Day, D. A. (1996) *FEBS Lett.* **398,** 155–158
69. Perazzolli, M., Dominici, P., Romero-Puertas, M. C., Zago, E., Zeier, J., Sonoda, M., Lamb, C., and Delledonne, M. (2004) *Plant Cell* **16,** 2785–2794
70. Navarre, D. A., Wendehenne, D., Durner, J., Noad, R., and Klessig, D. F. (2000) *Plant Physiol.* **122,** 573–582
71. Lindermayr, C., Saalbach, G., and Durner, J. (2005) *Plant Physiol.* **137,** 921–930
72. Vanin, A. F., Svistunenko, D. A., Mikoyan, V. D., Serezhenkov, V. A., Fryer, M. J., Baker, N. R., and Cooper, C. E. (2004) *J. Biol. Chem.* **279,** 24100–24107
73. Watts, R. N., and Richardson, D. R. (2002) *Eur. J. Biochem.* **290,** 693–699
74. Bright, J., Desikan, R., Hancock, J. T., Weir, I. S., and Neill, S. J. (2006) *Plant J.* **45,** 113–122
75. Vierstra, R. D. (2003) *Trends Plant Sci.* **8,** 135–142
76. Hellmann, H., and Estelle, M. (2002) *Science* **297,** 793–797
77. Callis, J., and Vierstra, R. D. (2000) *Curr. Opin. Plant Biol.* **3,** 381–386
78. Chiou, T. J., Aung, K., Lin, S. I., Wu, C. C., Chiang, S. F., and Su, C. L. (2006) *Plant Cell* **18,** 412–421
79. Lau, L. F., and Nathans, D. (1987) *Proc. Natl. Acad. Sci. U. S. A.* **84,** 1182–1186
80. Linial, M., Gunderson, N., and Groudine, M. (1985) *Science* **230,** 1126–1132
81. Shaw, G., and Kamen, R. (1986) *Cell* **46,** 659–667
82. Hershko, D. D., Robb, B. W., Wray, C. J., Luo, G. J., and Hasselgren, P. O. (2004) *J. Cell Biochem.* **91,** 951–961